DAMP HEAT STABILITY OF CHALCOPYRITE MINI-MODULES: EVALUATION OF SPECIFIC TEST STRUCTURES

Joachim Klaer, Reiner Klenk, Axel Boden, Axel Neisser, Christian Kaufmann, Roland Scheer, Hans-Werner Schock
Hahn-Meitner-Institut, Dep. Solar Energy, D-14109 Berlin, Germany

ABSTRACT

Damp heat stress (85% relative humidity at 85 °C) has been used to test long term stability of CIS thin film photovoltaic devices. Two CIS absorber types have been examined, $CuInS_2$ and $Cu(In,Ga)Se_2$. Module degradation is dominated by an increase of the series resistance R_s. In order to get information about the ZnO sheet resistance R_{sq} and the Mo/ZnO contact resistance R_c, which are the most important contributions to R_s, specially designed transmission-line test structures are used. Degradation of R_c strongly depends on the point of time when the second scribe for integrated series connection, P2, is made, while degradation of R_{sq} is strongly affected by the underlying absorber layer. Module-type solar cells without metal grid and complete mini-modules have been exposed to the same damp heat stress and yield additional information about degradation of other electrical parameters.

MOTIVATION

Long term stability is an essential issue for any commercial photovoltaic device. Exposure to damp heat is one of the time accelerated test procedures to simulate many years of out-door operation. Generally bare photovoltaic devices degrade when exposed to these test conditions so that encapsulation procedures are important for commercial devices. This encapsulation, however, contributes to production costs and may not be free of failure. Therefore it is desirable to make the naked device as insensitive to environmental influences as possible. In this paper we will focus on this strategy.

In order to increase the internal stability it is necessary to understand the origin of the degradation mechanisms. Each of the electrical parameters of a photovoltaic device, such as open circuit voltage V_{oc}, short circuit current I_{sc}, diode quality factor n, series resistance R_s, and shunt resistance R_p may degrade. Degradation of the latter three results in a degradation of the fill factor FF. All these parameters are obtained from I(V) measurements. The series resistance R_s, however, is composed of several contributions such as window layer (ZnO) resistance, back layer (molybdenum) resistance, semiconductor (CIS) resistance, contact resistance Mo/ZnO and contact resistance Mo/CIS. Unfortunately these contributions to R_s are not directly accessible from I(V) measurements.

As R_s plays an important role in degradation of CIS devices, further information about its contributions are needed. For $Cu(In,Ga)Se_2$ devices examinations on these questions have been performed by Wennerberg e.a. [1,2]. We have designed a test structure that gives access to the ZnO sheet resistance R_{sq} and the Mo/ZnO contact resistance R_c, which we consider the most important contributions concerning the increase of the series resistance during damp heat stress.

R_c is influenced by the way the second scribe P2 is performed. P2 is part of the integrated series connection and allows contact of ZnO to molybdenum. The ZnO layer is composed of a thin undoped layer (i-ZnO) followed by a thick layer of highly n-doped ZnO (n^+-ZnO). There are two possibilities to do P2: first, P2 is made prior to the deposition of undoped ZnO resulting in a Mo/i-ZnO interconnect, second, P2 is made after the deposition of the undoped ZnO, prior to n^+-ZnO, resulting in a Mo/n^+-ZnO interconnect.

From the electrical point of view one would favor the Mo/n^+-ZnO interconnect, but from the view of device processing the Mo/i-ZnO version is much less complicated, because both ZnO layers can be deposited directly one after the other not interrupted by the mechanical P2 scribe. So the knowledge of R_c as a function of stress is of particular interest.

EXPERIMENTAL

CIS technology

CIS based thin film photovoltaic devices with both, $CuInS_2$ and $Cu(In,Ga)Se_2$ absorbers have been investigated. For both types molybdenum coated float glass is used as substrate. $CuInS_2$ is deposited by a sequential process based on metal sputtering and rapid thermal sulfurization [3,4]. $Cu(In,Ga)Se_2$ absorbers are deposited by co-evaporation using a three stage process [5,6]. Subsequent processing is the same for both absorber types: CdS deposition from chemical bath and ZnO sputter deposition. Additional scribing steps are required for integrated series connection of modules: laser scribing of molybdenum (P1), mechanical scribing of CIS (P2) and mechanical scribing of ZnO + CIS (P3). Mini-modules having 7 integrated series connected cells are on 5x5 cm^2 substrates with an aperture area of about 18 cm^2.

The transmission-line test structure

Transmission-line structures allow separation of the contact resistance between two different layer materials

and the sheet resistance of one of them [7]. As first experiments indicated that ZnO on glass behaves differently from ZnO on $CuInS_2$ when exposed to damp heat, it was necessary to design a transmission-line structure that is processed identically to modules.

We developed a design that is depicted in Fig. 1. First, molybdenum is homogeneously sputtered onto the glass substrate and afterwards is structured by laser scribing (P1), thus generating the conductive fingers of the transmission-line structure (Mo1). This Mo1 is electrically isolated by the P1 grooves from the Mo2 areas between the fingers, which serve as back contact for solar cells. Next the CIS absorber layer is deposited onto the molybdenum followed by the CdS buffer layer. Now the second scribe (P2) is done mechanically in the middle of the underlying Mo1 fingers to allow contact of the subsequently deposited ZnO layer to the molybdenum fingers. Current flow from ZnO to Mo and vice versa is limited to these contacts, because the pn-junction between ZnO and CIS is isolating the ZnO layer from the highly conductive bottom Mo2 layer. Finally ZnO and CIS are mechanically removed from the sample except for the stripe in the middle of the sample, thereby defining the ZnO path and giving access to the molybdenum fingers.

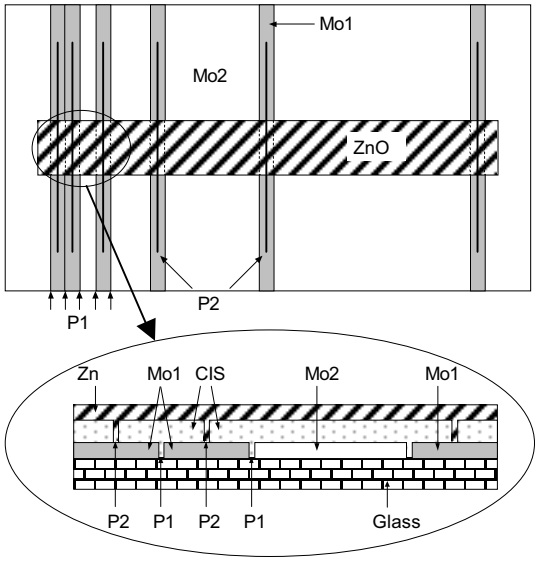

Fig. 1. Layout of the transmission-line test structure. The cross section shows an enlarged section of the left part of the structure. Resistances are measured from one Mo1 finger via the P2 contact to ZnO, through ZnO, via the next P2 contact to the next Mo1 finger. More details are described in the text.

Between two neighboring fingers the resistance measured is composed of the resistance of the Mo fingers, the Mo/ZnO contact resistance, and the sheet resistance of the ZnO stripe between the two fingers. Further measurements between fingers being separated from each other by increasing distances should result in increasing resistances because of the larger ZnO path length. In case of lateral homogeneity of all parameters involved, a plot of the measured resistances versus ZnO path length should show a linear curve. The slope of the curve gives the ZnO sheet resistance, the intersection of the curve with the y-axis gives the sum of the contact resistance and the Mo resistance (Fig. 2). In case the Mo resistance can be determined separately, the Mo/ZnO contact resistance can be extracted.

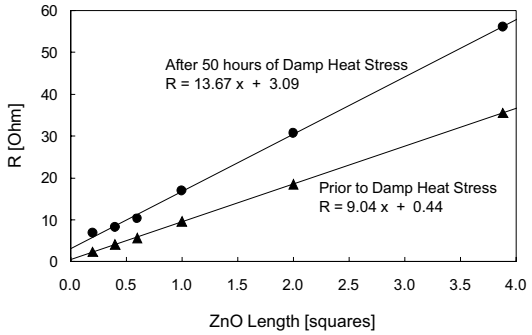

Fig. 2. Resistances as a function of the length of the ZnO stripe measured by the transmission-line structure given in Fig. 1. The ZnO stripe length is normalized to its width. The slope of the curves gives the ZnO sheet resistance R_{sq}, the extrapolation to zero ZnO length gives the sum of Mo/ZnO contact resistance R_c and the resistance of the Mo fingers. Prior to stress (lower curve) R_{sq} was 9.04 Ω/square and R_c was 0.44 Ω.

Solar cells are located on the same samples between the Mo1 fingers of the transmission-line structure. Their ZnO front contact is connected via a P2 groove to a neighboring molybdenum pad, a Mo1 finger. So like modules these solar cells have no metal grid. Their back contact is formed by the Mo2 areas. The 4 cells on each sample all have different lengths.

Damp heat stress

Time accelerated lifetime tests have been performed using damp heat stress in a climatic exposure test cabinet exposing the samples to 85% relative humidity at 85 °C. None of the samples has been encapsulated, thus the ZnO top layer is directly exposed to damp heat. The damp heat stress is extended up to 540 hours, repeatedly interrupted for measurements at room temperature.

RESULTS AND DISCUSSION

Transmission-line measurements

The resistance measured on the transmission-line samples was deconvoluted into ZnO sheet resistance R_{sq} and Mo/ZnO contact resistance R_c as explained above and shown in Fig. 2.

In Fig. 3 R_c is given as a function of damp heat stress time for a ZnO window layer deposited on $Cu(In,Ga)Se_2$.

There is a clearly different stress induced development of R_c depending on the interconnect version. For Mo/n^+-ZnO interconnects R_c remains up to one order of magnitude lower throughout the whole stress cycle compared to Mo/i-ZnO interconnects. The same applies in case of ZnO on $CuInS_2$ absorbers as shown earlier [8].

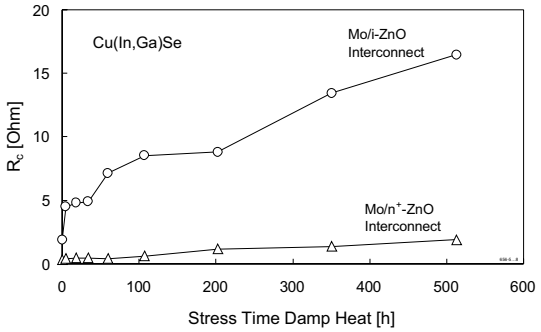

Fig. 3. Contact resistance Mo/ZnO as a function of stress time under damp heat condition for ZnO on Cu(In,Ga)Se_2 absorber layers.

The ZnO sheet resistance R_{sq} on CIS as a function of damp heat stress time is given in Fig. 4. The upper two curves show that R_{sq} on $CuInS_2$ increases much stronger than it does on Cu(In,Ga)Se_2, represented by the two lower curves. On both types of absorbers the same ZnO was used, sputtered under identical conditions. The different degradation of R_{sq} is believed to be due to different surface roughness of the absorber layers. The sequentially deposited $CuInS_2$ has a much rougher surface than the co-evaporated Cu(In,Ga)Se_2. A more detailed analysis concerning this difference is still in progress.

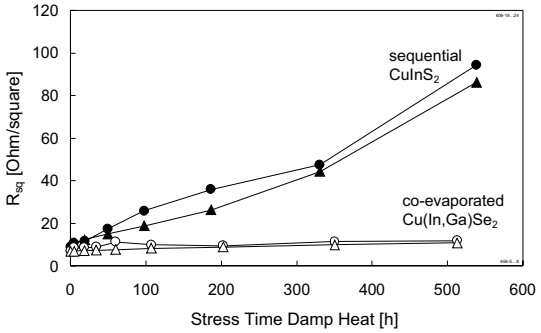

Fig. 4. Sheet resistance R_{sq} of ZnO on $CuInS_2$ (filled symbols) and Cu(In,Ga)Se_2 (open symbols) as a function of stress time under damp heat condition. R_{sq} degradation is independent from the interconnect type: Mo/i-ZnO (circles) or Mo/n^+-ZnO (triangles).

As expected the type of interconnect does not influence the degradation of R_{sq} on neither absorber. But there is a further difference between the two interconnect versions. In case of Mo/n^+-ZnO the measured resistances can easily be fitted by a straight line, an example of which is given in Fig. 2. This indicates good lateral homogeneity over the whole sample, which is a pre-requisite for deconvolution of R_{sq} and R_c as discussed above. In case of Mo/i-ZnO interconnects the measured resistances do not lie that nicely on a straight line. So the fitting, which is necessary to extract R_{sq} and R_c, is afflicted with much greater errors. Presumably for this reason the top curve in Fig. 3 is less smooth than the bottom curve.

As the n^+-ZnO layer, which is responsible for the conductivity of the ZnO, is identical for both types of interconnects, it is reasonable to assume that the inhomogeneities, observed in case of Mo/i-ZnO interconnects only, are due to lateral inhomogeneous contact resistances and caused by an i-ZnO layer that degrades inhomogeniously. Lateral inhomogeneous devices may become a problem especially for large area modules, because relatively small areas with poor performance, e.g. high series resistance, can deteriorate the whole device.

This deconvolution of R_s into R_{sq} and R_c is important for module design, concerning the cell length (distances between two neighboring P2 scribes). In case of Mo/i-ZnO interconnects a reduction of cell length has less influence on the R_s, since only R_{sq} is scaling down and for short cells R_c will dominate; longer cells will be favorable here. On the other hand R_c may be neglected for the module design in case of Mo/n^+-ZnO interconnects.

The most important loss mechanism for CIS devices throughout damp heat stress is the increase of R_s, especially for long stress times. So improvement of the window layer stability and choice of the more laborious version with Mo/n^+-ZnO interconnects has the greatest impact on device stability against damp heat stress.

Solar cells and modules

Together with the transmission-line structures the solar cells without grid that are on the same samples and complete mini-modules have also been measured repeatedly. There are 4 differently sized cells on each transmission-line sample. The width of 5 mm is the same for all these cells but they differ in length (direction of current flow in the ZnO). We will take a closer look at the two medium sized cells having ZnO lengths of 3 and 8 mm and cell areas of 0.15 and 0.4 cm^2, respectively.

In Fig. 5 the decrease of the efficiency and in Fig. 6 the increase of the series resistance are given as a function of damp heat stress time for single module-type solar cells and complete mini-modules. The correspondence of efficiency decrease to series resistance increase indicates that device degradation is to a great extent due to series resistance. The smallest cells (0.15 cm^2) with only 3 mm current transport length in the ZnO are more stable than cells with 8 mm path length (0.40 cm^2). This underlines the contribution of ZnO sheet resistance R_{sq} to series resistance degradation because the longer the ZnO path length the stronger the degradation while the contact geometry is identical for both cell sizes.

The strongest degradation is observed for complete mini-modules. The ZnO length in this case is 6 mm, so

there must be additional contributions to degradation of R_s in the case of mini-modules that are not present in the single cells. This may be due to the fact that modules and transmission line samples have been processed in different batches at different times. There will be additional experiments to gain more information.

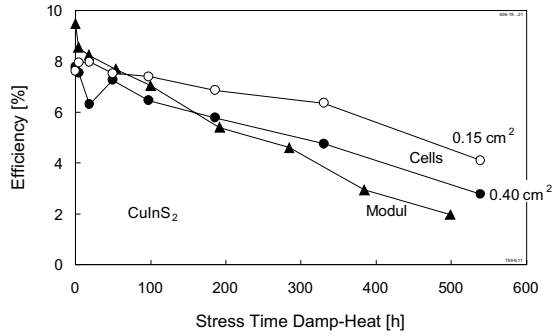

Fig. 5. Efficiency degradation due to damp heat stress of $CuInS_2$ module-type solar cells without grid (circles) and complete mini-modules (triangles).

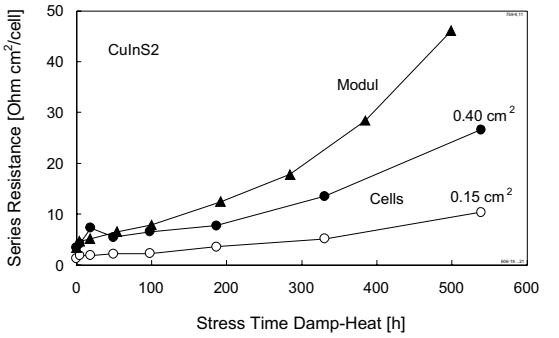

Fig. 6. Increase of the series resistance of the same devices as shown in Fig. 5.

Besides the series resistance R_s, the diode quality factor n also increases due to damp heat stress, thus also contributing to the degradation of the fill factor, as shown recently [8].

SUMMARY AND CONCLUSION

The ZnO sheet resistance R_{sq} and the Mo/ZnO contact resistance R_c as major contributions to the series resistance R_s of CIS based photovoltaic thin film devices were measured by means of a specially designed transmission-line test structure that is equally processed compared to modules. Both contributions increase upon unprotected exposure to damp heat stress.

The increase of R_{sq} depends on the absorber layer. ZnO on $Cu(In,Ga)Se_2$ is more stable than on $CuInS_2$. This difference could be attributed to the smoother surface of the co-evaporated $Cu(In,Ga)Se_2$ compared to sequentially deposited $CuInS_2$.

The increase of the R_c strongly depends on the interconnect type. In case of Mo/n^+-ZnO interconnects R_c is significantly less sensitive to damp heat stress compared to the Mo/i-ZnO interconnect version. For R_{sq}, however, there is no difference for both interconnect versions.

Non-encapsulated CIS solar cells without grid and complete mini-modules show degradation when exposed to damp heat stress. The decrease in efficiency is to a great part due to increase of series resistance.

More experiments will be performed to prove the correlation between absorber surface roughness and ZnO sheet resistance degradation. Also there will be examinations on additional contributions to degradation of R_s of mini-modules that still cannot completely be explained by R_s of single module-type cells and R_c and R_{sq} of transmission-line test structures.

ACKNOWLEDGEMENTS

The authors want to thank E. Müller, B. Bunn, N. Blau, C. Kelch, M. Kirsch and T. Münchenberg for sample preparation and M. González for stress tests and measurements.

REFERENCES

[1] J. Wennerberg, J. Kessler, L.Stolt, "Degradation mechanism of $Cu(In,Ga)Se_2$-based thin film PV modules", *Proc. 16th Europ. Photovolt. Solar Energy Conf.*, Glasgow, 2000, pp. 309-312.

[2] J. Wennerberg, J. Kessler, L.Stolt, "$Cu(In,Ga)Se_2$-based thin-film photovoltaic modules optimized for long-term performance", *Solar Energy Materials & Solar Cells* **75**, 2003, pp.47-55.

[3] J. Klaer, J. Bruns, R. Henninger, M. Weber, K. Ellmer, R. Klenk, R. Scheer, D. Bräunig, "$CuInS_2$ solar cells from sputtured CuIn precursors reacted in sulphur vapour", *Proc. 14th Europ. Photovolt. Solar Energy Conf.*, Barcelona, 1997, pp.1307-1310.

[4] K. Siemer, J. Klaer, I. Luck, J. Bruns, R. Klenk, D. Bräunig, "Efficient $CuInS_2$ solar cells from a rapid thermal process (RTP)", *Solar Energy Materials & Solar Cells* **67**, 2001, pp.159-166.

[5] A. Neisser, C. A. Kaufmann, M.A. Kroon, R. Klenk, R. Scheer, "Flexible $Cu(In,Ga)Se_2$ solar cells for space applications", *Proc. 3rd World Conf. Photovolt. Energy Conversion,* Osaka, 2003, pp. 458-460.

[6] A.M. Gabor, J.R. Tuttle, D.S. Albin, M.A. Contreras, "High-efficiency $CuIn_xGa_{1-x}Se_2$ solar cells made from $(In_x,Ga_{1-x})_2Se_3$ precursor films", *Appl. Phys. Lett.* **65**, 1994, pp.198-200.

[7] H.H. Berger, "Models for contacts to planar devices", *Solid-State Electronics* **15**, 1972, pp.145-158.

[8] J. Klaer, R. Scheer, R. Klenk, A. Boden, C. Köble, "Stress behaviour of $CuInS_2$ thin film PV-modules studied by a specific test structure", *19th Europ. Photovolt. Solar Energy Conf.*, Paris, 2004, pp.1847-1850.